

²The target mechanism was designed by C. R. Flatau (to be published).

³J. B. Cummings, J. Hudis, A. M. Poskanzer, and S. Kaufman, Phys. Rev. 128, 2392 (1962).

⁴J. G. V. Taylor and J. S. Merrit, Can. J. Phys. 40, 926 (1962).

⁵B. Cork, W. A. Wenzel, and C. W. Causey, Jr., Phys. Rev. 107, 859 (1957).

ANTIPROTON AND KAON ELASTIC SCATTERING AT HIGH ENERGIES*

K. J. Foley, S. J. Lindenbaum, W. A. Love, S. Ozaki, J. J. Russell, and L. C. L. Yuan
Brookhaven National Laboratory, Upton, New York
(Received 7 November 1963)

This Letter reports measurements of differential elastic cross sections for \bar{p} - p scattering at 7.2, 8.9, 10.0, and 12.0 BeV/c, for K^+ - p at 6.8, 9.8, 12.8, and 14.8 BeV/c, and for K^- - p at 7.2 and 9.0 BeV/c. For \bar{p} - p the range of four-momentum transfer squared, t , covered is $0.03 < -t < 0.6$ (BeV/c)² and for K^\pm - p , $0.03 < -t < 1.1$ (BeV/c)². There is some evidence that the \bar{p} - p system does not exhibit the "Regge-pole" shrinkage observed in the p - p system, while the behavior of the K^+ - p system is consistent with that of p - p . Data on K^- - p are not sufficient to draw shrinkage conclusions.

All measurements were made using the hodoscopes and data handling systems employed to

measure π^\pm and p scattering.¹ They include cross sections at small angles, obtained by measuring the momentum of the scattered particle to establish elasticity, and cross sections for $|t| > 0.25$ (BeV/c)² measured by observing the angular correlation of scattered and recoil particles. These have been combined using the relative normalization factor deduced previously for π^\pm and p scattering. Corrections were applied to the two sets of data to allow for K^\pm decay; these corrections were calculable to an accuracy of a few percent and introduce, therefore, no appreciable additional error.

The resulting differential cross sections with their appropriate t values, as well as values of

Table I. The experimental cross sections. Under each momentum are given the total elastic cross section, the ratio of the elastic to the total cross section, the result of extrapolating the measured values of $d\sigma/dt$ to $t=0$, and a table of the t values and cross sections. The results of the magnetic analysis system are marked with an asterisk. Values of $d\sigma/dt$ are given in mb/(BeV/c)², and the units of t are (BeV/c)². In addition to the errors given, there is an over-all systematic scale uncertainty of $\pm 5\%$ for \bar{p} - p , $\pm 7\%$ for K^\pm - p , and a relative normalization uncertainty of $\pm 3\%$ between the two sets of data.

P	\bar{p} - p							
	7.2 BeV/c		8.9 BeV/c		10.0 BeV/c		12.0 BeV/c	
σ_{el}	13.79 \pm 1.00 mb		13.89 \pm 0.35 mb		14.6 \pm 3.3 mb		11.59 \pm 0.41 mb	
σ_{el}/σ_t	0.226 \pm 0.017		0.238 \pm 0.009		0.257 \pm 0.058		0.213 \pm 0.010	
$d\sigma/dt(0)$	181 \pm 16		178 \pm 5.1		173 \pm 47		147 \pm 6.4	
	$-t$	$d\sigma/dt$	$-t$	$d\sigma/dt$	$-t$	$d\sigma/dt$	$-t$	$d\sigma/dt$
	*0.026	131 \pm 20	*0.024	127.0 \pm 6.3	*0.030	122 \pm 31	*0.043	80.9 \pm 4.2
	*0.037	84 \pm 18	*0.038	114.0 \pm 5.2	*0.049	75 \pm 23	*0.070	62.1 \pm 3.3
	*0.052	113 \pm 18	*0.058	83.9 \pm 3.9	*0.074	82 \pm 18	*0.105	38.1 \pm 2.3
	*0.070	72 \pm 14	*0.082	57.0 \pm 3.1	*0.105	56 \pm 15	*0.149	24.9 \pm 1.8
	*0.089	39.0 \pm 11.1	*0.110	43.9 \pm 2.8	*0.140	27 \pm 12	*0.198	12.2 \pm 1.3
	*0.109	47.9 \pm 8.2	*0.138	32.6 \pm 2.2	*0.176	19 \pm 10	*0.249	7.15 \pm 0.95
	0.272	4.95 \pm 0.44	*0.172	20.5 \pm 1.6			0.268	4.09 \pm 0.44
	0.349	2.01 \pm 0.25	0.264	5.23 \pm 0.42			0.343	1.96 \pm 0.27
	0.434	0.42 \pm 0.12	0.338	2.48 \pm 0.24			0.428	0.583 \pm 0.132
	0.524	0.24 \pm 0.09	0.422	0.77 \pm 0.13			0.517	0.190 \pm 0.091
			0.508	0.282 \pm 0.077				
			0.602	0.091 \pm 0.045				

(Continued on p. 504.)

Table I (continued).

		K^+-p							
P		6.8 BeV/c		9.8 BeV/c		12.8 BeV/c		14.8 BeV/c	
σ_{el}		3.48 \pm 0.43 mb		3.34 \pm 0.17 mb		3.34 \pm 0.15 mb		3.41 \pm 0.17 mb	
σ_{el}^+/σ_t		0.189 \pm 0.024		0.182 \pm 0.11		0.182 \pm 0.010		0.185 \pm 0.011	
$d\sigma^-/dt(0)$		19.7 \pm 4.3		19.7 \pm 1.5		22.0 \pm 1.4		22.3 \pm 1.6	
		$-t$	$d\sigma/dt$	$-t$	$d\sigma/dt$	$-t$	$d\sigma/dt$	$-t$	$d\sigma/dt$
		0.251	4.81 \pm 0.34	*0.049	14.74 \pm 1.56	*0.050	16.43 \pm 1.31	*0.066	14.37 \pm 1.06
		0.321	2.93 \pm 0.24	*0.071	13.20 \pm 1.38	*0.083	12.76 \pm 0.99	*0.111	9.61 \pm 0.84
		0.399	2.11 \pm 0.18	*0.098	10.15 \pm 1.08	*0.120	8.47 \pm 0.87	*0.161	7.81 \pm 0.77
		0.481	1.46 \pm 0.15	*0.133	8.37 \pm 0.97	*0.166	7.21 \pm 0.67	*0.222	5.03 \pm 0.57
		0.569	0.944 \pm 0.117	*0.173	7.87 \pm 0.94	*0.224	5.05 \pm 0.53	0.290	3.23 \pm 0.23
		0.663	0.671 \pm 0.100	*0.212	4.36 \pm 0.78	0.277	3.80 \pm 0.24	*0.300	3.63 \pm 0.41
		0.762	0.331 \pm 0.072	0.266	4.12 \pm 0.29	*0.291	3.62 \pm 0.46	0.371	2.00 \pm 0.16
		0.867	0.266 \pm 0.071	0.340	2.69 \pm 0.21	0.354	2.25 \pm 0.17	*0.389	1.75 \pm 0.30
		0.977	0.219 \pm 0.057	0.423	1.58 \pm 0.14	0.441	1.43 \pm 0.12	0.462	1.23 \pm 0.11
		1.091	0.117 \pm 0.049	0.510	1.09 \pm 0.12	0.531	0.652 \pm 0.085	0.558	0.805 \pm 0.086
		1.193	0.058 \pm 0.042	0.605	0.716 \pm 0.094	0.630	0.521 \pm 0.071	0.661	0.451 \pm 0.067
				0.707	0.300 \pm 0.062	0.736	0.235 \pm 0.046	0.774	0.181 \pm 0.045
				0.816	0.270 \pm 0.055	0.849	0.112 \pm 0.035	0.896	0.153 \pm 0.040
				0.931	0.162 \pm 0.048	0.971	0.060 \pm 0.025	1.024	0.115 \pm 0.035
				1.051	0.043 \pm 0.027	1.099	0.054 \pm 0.019	1.160	0.069 \pm 0.028
		$K^- - p$							
P		7.2 BeV/c				9.0 BeV/c			
σ_{el}		4.23 \pm 0.85 mb				3.95 \pm 0.78 mb			
σ_{el}^+/σ_t		0.169 \pm 0.034				0.161 \pm 0.032			
$d\sigma/dt(0)$		38.9 \pm 11.0				37.5 \pm 10.8			
		$-t$	$d\sigma/dt$	$-t$	$d\sigma/dt$	$-t$	$d\sigma/dt$	$-t$	$d\sigma/dt$
		0.271	3.17 \pm 0.27	0.265	3.17 \pm 0.26	0.340	1.77 \pm 0.17	0.423	0.880 \pm 0.105
		0.348	1.86 \pm 0.18	0.510	0.582 \pm 0.085	0.605	0.310 \pm 0.061	0.707	0.161 \pm 0.045
		0.434	1.16 \pm 0.13	0.619	0.384 \pm 0.074	0.815	0.139 \pm 0.038	0.929	0.100 \pm 0.032
		0.523	0.461 \pm 0.082	0.722	0.105 \pm 0.041	1.049	0.017 \pm 0.016	1.176	0.060 \pm 0.032
		0.619	0.384 \pm 0.074	0.831	0.107 \pm 0.043				
		0.722	0.105 \pm 0.041	0.947	0.079 \pm 0.040				
		0.831	0.107 \pm 0.043	1.065	0.060 \pm 0.030				
		0.947	0.079 \pm 0.040	1.190	0.082 \pm 0.034				
		1.065	0.060 \pm 0.030						
		1.190	0.082 \pm 0.034						

$(d\sigma/dt)_t=0$ and σ_{el} obtained from fits to the data, are given in Table I. The errors shown are predominantly statistical (7-50%) but include estimates of errors due to counter size uncertainty (1%) and t -value uncertainty (11% for \bar{p} , 5% for K^+ , and 8% for K^-). An additional 5% absolute scale uncertainty applies to the \bar{p} data, 7% to the K^\pm data, and a further 3% relative scale error to the results of the magnetic analysis experiment, associated with the relative normalization.

After combining the data, fits were made of the form

$$[\sigma_t(12)/\sigma_t(p)]^2 d\sigma/dt = e^{a+bt+ct^2}.$$

The factor multiplying $d\sigma/dt$ is inversely proportional to $(d\sigma/dt)_{opt}$ and is unity at 12 BeV/c. For K^\pm it has been placed equal to 1 since there is no significant variation of σ_t with energy²; for $\bar{p}-p$, values of σ_t have been taken from the work of Lindenbaum *et al.*³ Data points from the highest and the lowest momentum measured, as well as values of a , b , and c obtained from the fits, are shown in Fig. 1. For $\bar{p}-p$ no statistical improvement resulted from the use of c ; hence a two-parameter fit was used.

The average slope of the $d\sigma/dt$ curves at low t differs significantly for the different incident particles, being largest for $\bar{p}-p$, intermediate and

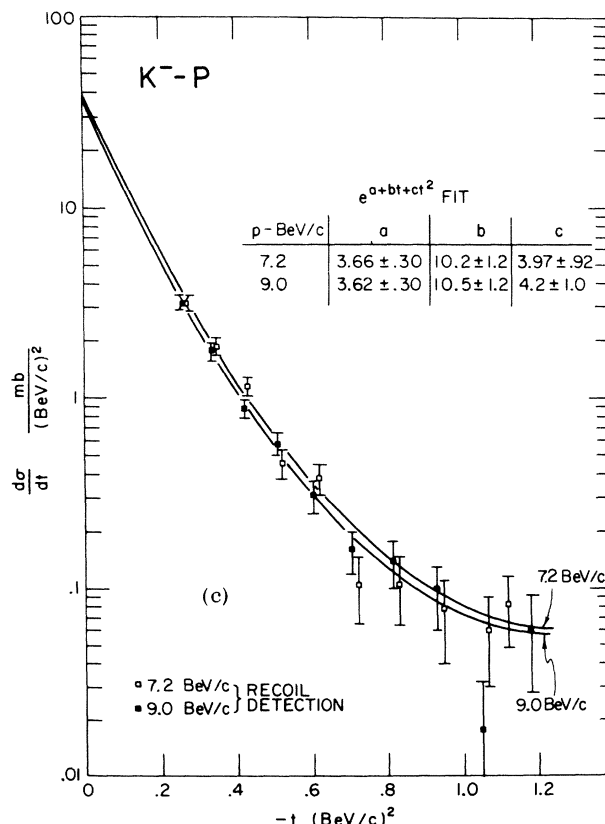
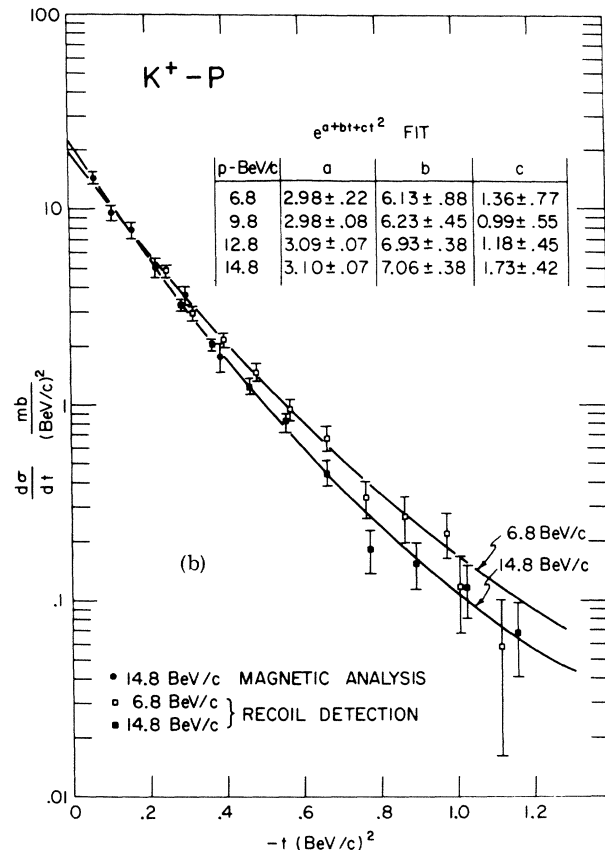
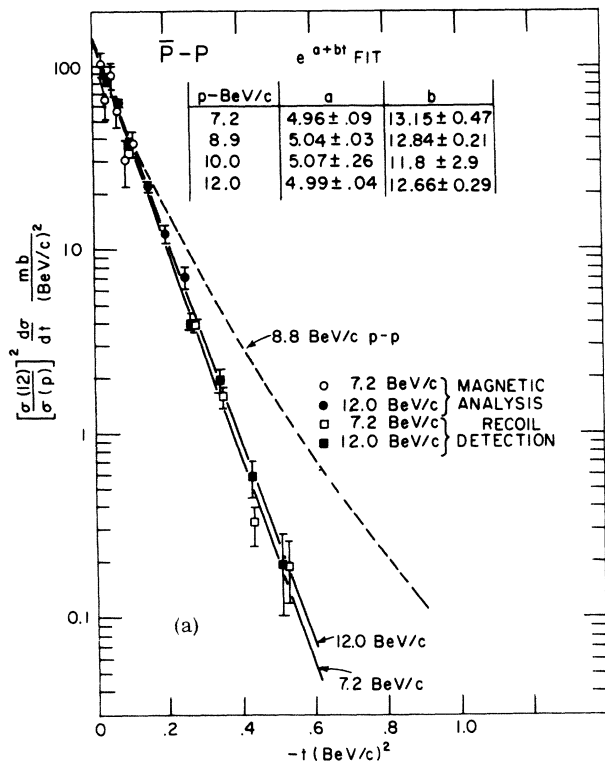


FIG. 1. Differential cross sections for the highest and lowest momenta measured. In addition to the errors shown, there is a systematic scale uncertainty of +5% for $\bar{p}-p$, 7% for $K^\pm-p$, and a 3% relative normalization uncertainty between magnetic analysis and recoil detection data. (a) $\bar{p}-p$; the dashed line is a $p-p$ curve at a comparable momentum. (b) K^+-p . (c) $K^- -p$.

comparable for $\pi^\pm-p$, $p-p$,¹ and $K^- -p$, and smallest for $K^+ -p$, indicating that the effective interaction radii differ accordingly.

Values of $(d\sigma/dt)_{t=0}$ for $\bar{p}-p$ coincide with the optical-theorem prediction for each momentum, but the errors in $\sigma_t(\bar{p}-p)$ ³ and the present experiment combined would not exclude as much as a 16% difference from the optical cross sections. For K^+ scattering, a 20% excess over the optical-theorem prediction is indicated by the data, but this value is near the upper limit of the combined errors of $\sigma_t(K^+-p)$ ² and the present measurements. Similarly, an 18% excess is indicated for K^- scattering but is within the limit of the combined experimental errors.

Using the fits, values of cross sections at intermediate t values have been obtained; the errors used on these interpolated points were obtained from the experimental errors on adjacent measurements, and the total number of interpolated points does not exceed the number of experi-

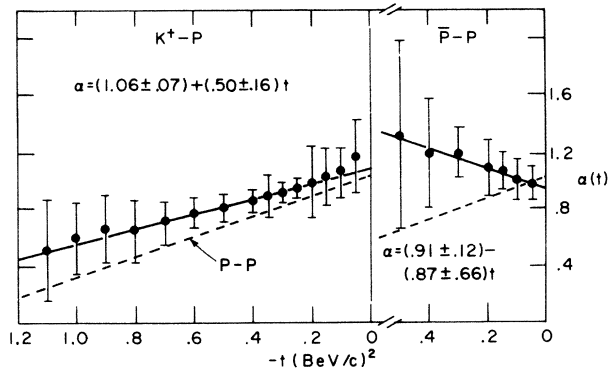


FIG. 2. $\alpha(t)$ versus $-t$; for comparison, the p - p trajectory from reference 1 is shown.

mental data points. From a logarithmic plot of the interpolated values versus $\ln s$, values of $\alpha(t)$ for a single Regge-pole representation of K^+ and \bar{p} scattering have been obtained, using

$$\ln(d\sigma/dt) = F(t) + 2[\alpha(t) - 1] \ln s,$$

where s is the square of the energy in the center-of-mass system.

As there appears to be little agreement with

any specific theoretical scheme presently, the above simple representation of the data seems preferable to anything more elaborate. Values of $\alpha(t)$ thus obtained are shown in Fig. 2; the α curve for p - p scattering is also shown.

From Fig. 2 as well as from the experimental cross sections, one can see that \bar{p} - p scattering does not appear to exhibit the shrinkage observed in p - p scattering; in fact, the best fit indicates an expansion 1.3 standard deviations from no shrinkage and 2.5 standard deviations from the p - p shrinkage. K^+ - p scattering, on the other hand, can be described by a straight-line trajectory having a slope $(66 \pm 21)\%$ that of the p - p trajectory.

*Work performed under the auspices of the U. S. Atomic Energy Commission.

¹K. J. Foley, S. J. Lindenbaum, W. A. Love, S. Ozaki, J. J. Russell, and L. C. L. Yuan, Phys. Rev. Letters 10, 376, 543 (1963); 11, 425 (1963).

²W. F. Baker, R. L. Cool, E. W. Jenkins, T. F. Kycia, R. H. Phillips, and A. L. Read, Phys. Rev. 129, 2285 (1963).

³S. J. Lindenbaum, W. A. Love, J. A. Niederer, S. Ozaki, J. J. Russell, and L. C. L. Yuan, Phys. Rev. Letters 7, 185 (1961).

DEUTERON PRODUCTION IN pp COLLISIONS*

J. Chahoud and G. Russo

Istituto di Fisica dell'Università, Bologna, Italy
and Istituto Nazionale di Fisica Nucleare, Sezione di Bologna, Italy

and

F. Selleri

Laboratory of Nuclear Studies, Cornell University, Ithaca, New York
(Received 7 November 1963)

In a recent note Cocconi *et al.*¹ have shown that the total cross section for the reaction



is likely to present a maximum at total c. m. energy $E^* = 2.9$ BeV, beyond the well-established maximum at $E^* = 2.16$ BeV. The above authors observed also that these values of E^* correspond almost exactly to the masses of the first and fourth pion-nucleon resonances plus a nucleon mass.

It is the aim of the present note to point out that these facts, together with the nonappearance of the second and third πN resonances, are explained by a simple model of deuteron produc-

tion.

As the reaction



in the same energy region is well explained by the one-pion exchange (O. P. E.) model,² we assume that Reaction (1) is generated by the O.P.E. mechanism followed by an interaction in the final state, which binds p and n into a deuteron.

This picture corresponds to the diagram shown in Fig. 1. First we show that the fact that p and n bind together in a deuteron freezes the three-body kinematics of the intermediate state in such a way that there is almost a one-to-one correspondence between the total c. m. energy squared